Mechanistic Basis for Nonlinear Kinetics of Aldehyde Reduction Catalyzed by Aldose Reductase†

C. E. Grimshaw,* M. Shahbaz,‡ and C. G. Putney

Division of Biochemistry, Department of Molecular and Experimental Medicine, Research Institute of Scripps Clinic, Scripps Clinic and Research Foundation, La Jolla, California 92037

Received August 21, 1989; Revised Manuscript Received July 2, 1990

ABSTRACT: Bovine kidney aldose reductase (ALR2) displays substrate inhibition by aldehyde substrates that is uncompetitive versus NADPH when allowance is made for nonenzymic reaction of the aldehyde with the adenine moiety of NADPH. A time-dependent increase in substrate inhibition observed in product versus time plots for reduction of short-chain aldoses containing an enolizable α-proton, but not for *p*-nitrobenzaldehyde, is shown to be consistent with a model in which rapidly reversible inhibition due to formation of the dead-end E·NADP·glycolaldehyde complex is combined with the formation at the enzyme active site of a tightly-bound covalent NADP–glycolaldehyde adduct. Quantitative analysis of reaction time courses for ALR2-catalyzed reduction of glycolaldehyde using NADPH or the 3-acetylpyridine analogue, (AP)ADPH, yields values of the forward and reverse rate constants for ALR2-mediated adduct formation that agree with the values determined in the absence of glycolaldehyde turnover. Substrate inhibition is only partial, indicating that reaction can occur via an alternate pathway at high [glycolaldehyde]. Kinetic evidence for a slow isomerization of the E·NADP complex at pH 8.0 is used to explain the similar V/E_t values observed for glycolaldehyde reduction at pH 7.0 using NADPH, (AP)ADPH, and the hypoxanthine analogue N(Hx)DPH. The practical implications of these results for kinetic studies of aldose reductase are discussed.

Recently, we demonstrated the existence of two forms of bovine kidney aldose reductase (ALR2;[1] alditol–$NADP^+$ 1-oxidoreductase; E.C. 1.1.1.21), an activated and an unactivated enzyme form, and showed that nonlinear double-reciprocal plots of $1/v_i$ versus 1/[aldehyde] for reduction of a variety of aldehyde substrates could be explained in terms of the separate contributions of these two enzyme forms to the observed rate (Grimshaw et al., 1989). However, it is surprising in view of the apparent immunologic, kinetic, and structural similarity of ALR2 isolated from several mammalian species (Conrad & Doughty, 1982; Mathur & Grimshaw, 1986; Morjana & Flynn, 1989; Bohren et al., 1989; Nishimura et al., 1989; Schade et al., 1990) that recognition of the nonlinear kinetic properties of the ALR2-catalyzed reaction has not been more widespread.

Previously we showed that substrate inhibition of ALR2 by high concentrations of glycolaldehyde or glyceraldehyde can lead to a rapid ($t_{1/2} \approx 10$ s) decrease in the initial steady-state velocity to a slower, limiting steady-state velocity (McKercher et al., 1985; Grimshaw, 1986, 1987), similar to the results reported for pyruvate inhibition of lactate dehydrogenase (Gutfreund et al., 1968; Burgner et al., 1978). Because this rapid decay of the reaction rate becomes significant over the same aldehyde concentration range in which *activation* would otherwise be detected due to the contribution of the more active enzyme form (Grimshaw et al., 1989), we reasoned that substrate inhibition might explain why nonlinear double-reciprocal plots for ALR2 are not more commonly observed.

Although product versus time plots for ALR2-catalyzed reduction of glyceraldehyde display a time-dependent decay in rate similar to that seen for glycolaldehyde, spectroscopic evidence suggests that adduct formation with the three-carbon aldoses may be complicated by a second reaction that is dependent on the stereochemistry at the α-carbon (Grimshaw, 1989). In addition, because the stereospecificity of ALR2 for the glyceraldehyde enantiomers appears to change under certain conditions (Del Corso et al., 1989; Grimshaw et al., 1989), we chose to study the simple two-carbon aldose, glycolaldehyde.

In the preceding paper (Grimshaw et al., 1990), we show that covalent adduct formation between glycolaldehyde enol and the oxidized nucleotide cofactor can indeed occur at the

† This work was supported by a grant to C.E.G. from the National Institute for Diabetes and Digestive and Kidney Diseases (DK 32218) and by the Olive H. Whittier Fund. Support for the VAX 11/750 in the General Clinical Research Center, Scripps Clinic and Research Foundation, was provided by the Division of Research Resources (Grant RR 00833) from the National Institutes of Health. This is publication number 5170-MEM from the Research Institute of Scripps Clinic, Scripps Clinic and Research Foundation.

* Address correspondence to this author.

‡ Present address: Progenix, Inc., La Jolla, CA 92037.

[1] The nomenclature for aldose reductase (ALR2) was recommended by the First International Workshop on Aldehyde Dehydrogenase and Aldehyde Reductase, held in Bern, Switzerland, on July 12–14, 1982 (Turner & Flynn, 1982). Abbreviations: Na_2EDTA, disodium ethylenediaminetetraacetate; Mops, 3-(*N*-morpholino)propanesulfonic acid; NAD^+, β-nicotinamide adenine dinucleotide; NADH, reduced form of NAD^+; $NADP^+$, β-nicotinamide adenine dinucleotide phosphate; NADPH, reduced form of $NADP^+$; N(Hx)DP^+, β-nicotinamide hypoxanthine dinucleotide phosphate; N(Hx)DPH, reduced form of N(Hx)DP^+; (AP)ADP^+, β-3-acetylpyridine adenine dinucleotide phosphate; (AP)ADPH, reduced form of (AP)ADP^+; (AP)AD^+, β-3-acetylpyridine adenine dinucleotide; NADP–ald or simply "adduct", the covalent adduct [1,4-dihydro-4-(1-hydroxy-2-oxoethyl)nicotinamide adenine dinucleotide phosphate] resulting from reaction of glycolaldehyde with $NADP^+$; E·NADP·ald, the ternary dead-end complex of ALR2 with $NADP^+$ and glycolaldehyde; E·NADP–ald, the *binary* E·adduct complex [similar nomenclature is used for adduct and enzyme complexes containing (AP)ADP^+ and N(Hx)DP^+]. Fluorescence data are given as ${}_{ex}F_{emit}$ with λ_{max} for excitation (λ_{max}^{ex}) and emission (λ_{max}^{emit}) shown as preceding and following subscripts, respectively.

0006-2960/90/0429-9947$02.50/0

ALR2 active site, thus satisfying the first requirement of the lactate dehydrogenase substrate inhibition model (Burgner & Ray, 1974, 1978). In this paper we examine the mechanistic basis for the nonlinear kinetics of glycolaldehyde reduction catalyzed by bovine kidney ALR2. Through a detailed kinetic analysis of the product versus time plots, substrate inhibition by glycolaldehyde is shown to be consistent with a modification of the model proposed in the preceding paper (Grimshaw et al., 1990). In addition, data are presented that clearly rule out the isomerization of free enzyme previously suggested as the rate-determining step in the forward reaction for aldehyde reduction (Grimshaw et al., 1989) and which instead suggest that isomerization of the E·NADP complex is kinetically significant at pH 8. The practical consequences of these results for kinetic studies of ALR2 are discussed.

Experimental Procedures

Materials. The materials and general methods have been described in the preceding paper (Grimshaw et al., 1990).

Standard Assay. Bovine kidney ALR2 was assayed by measuring, with a Beckman DU monochromator, Gilford 252 optical density converter, and Linseis 2025 strip chart recorder, the rate of enzyme-dependent decrease in A_{340nm} by using ϵ = 6220 M^{-1} cm^{-1} (P-L Biochemicals, 1961). Assays were performed at 25 °C in 1.0-cm path length quartz cuvettes containing 10 mM glycoaldehyde and 160 μM NADPH in a final volume of 1.0 mL of MOPSE buffer (50 mM Mops and 0.1 mM Na_2EDTA, pH 7.0). Temperature was maintained to within ±0.1 °C with a thermostated water bath and thermospacers. The concentration of ALR2 was determined as described previously (Grimshaw et al., 1989, 1990). Turnover number (V/E_t) is expressed as (μmol of product/s)/μmol of ALR2 active sites in units of s^{-1}.

Kinetic Studies. Initial rate and product versus time experiments at saturating NADPH (100 μM) or (AP)ADPH (100 μM) were conducted at 15 or 25 °C by monitoring the decrease in A_{340nm} or A_{363nm} (ϵ_{363nm} = 8800 M^{-1} cm^{-1}; Hermes et al., 1984) by using the apparatus described above for the standard assay. For NADPH or (AP)ADPH concentrations in the 1–10 μM range, the rate of enzyme-dependent decrease in fluorescence of free NADPH or (AP)ADPH ($_{365}F_{480}$; slits 2 nm excitation, 10 nm emission) was measured with a Perkin-Elmer 650-40 spectrofluorometer, Xe light source, and Hitachi 057 X-Y recorder. Assays were performed in quartz 1.0-cm^2 cuvettes in a final volume of 1.0 mL of MOPSE buffer (pH 7.0, unless otherwise indicated) with a full-scale deflection calibrated to equal a 1 μM change in NADPH or (AP)ADPH. Reactants were preincubated in MOPSE buffer at 15 or 25 °C, and the reaction was started by addition of a fixed volume of glycolaldehyde stock solution (at the same temperature). For initial velocity studies of the reverse reaction at pH 8.0 (ethylene glycol oxidation), the increase in $_{365}F_{480}$ was monitored (slits; 10 nm excitation and emission). Due to the unfavorable equilibrium and the low $NADP^+$ concentrations (0.5–4 μM), a full-scale deflection equivalent to 0.15 μM NADPH was used. Reactions were routinely monitored for 0.5–5 min, and the initial rates (dA/dt or dF/dt), estimated either directly by eye or by linear extrapolation of plots of $[P]/t$ against t to $t = 0$ (Alberty & Koerber, 1957), were corrected for the background rate (≤5%) detected in the absence of glycolaldehyde. Product versus time data (up to 10 min duration) were fitted to eq 1 by the nonlinear least-squares program supplied as part of the BMDP statistical software package (Dixon, 1988):

$$[P] = v_{lim}t + [(v_0 - v_{lim})/k'](1 - e^{-k't}) \quad (1)$$

where v_0 and v_{lim} are the initial and limiting steady-state velocities, respectively, and k' is the first-order rate constant for transition between v_0 and v_{lim}.

Reaction of Glycolaldehyde with Adenine-Containing Nucleotides. The reaction time course was monitored by measuring the spectrum (225–400 nm) at fixed time intervals (5–600 s) with a Hewlett-Packard 8450A double-beam diode array spectrophotometer. Assays were conducted in tandem-compartment quartz cells (total path length = 0.9 cm) preincubated at 25 °C in a custom-designed water-jacketed cell holder. One side of both the sample and reference cells contained nucleotide and the other side contained glycolaldehyde; the concentration of buffer (50 mM sodium phosphate and 0.1 mM Na_2EDTA, pH 7.0) was the same in all compartments. The contents of the sample cell were mixed to start the reaction, and the digitized initial spectrum [$spectrum_{t=0}$ = (sample − reference)$_{t=0}$], measured within 5 s of mixing, was stored and subtracted from each subsequent spectrum, thus generating a time course of difference spectra ($spectrum_t - spectrum_{t=0}$). Digital absorbance data averaged over the peak of maximum absorbance change (272 ± 2 nm) were plotted versus time, and the initial rate was determined as described above. Upon completion, the process was repeated by mixing the reference cell contents and the final spectrum was checked for complete cancellation of the observed absorbance changes.

Rate of Adduct Decomposition and Estimation of Adduct Stoichiometry. The rate constant for E·adduct decomposition (k'_r) was determined from the time course for recovery of enzyme activity. An aliquot (40 μL) of equilibrated E·adduct mixture (7.8 μM ALR2, 50 mM glycolaldehyde, and 25 μM $NADP^+$ or $(AP)ADP^+$ incubated at 15 °C for 45 min) was diluted into a 1.0-mL assay mixture (final [ALR2] = 0.31 μM, 160 μM NADPH, 5 mM glycolaldehyde, MOPSE buffer, 15 °C), and the reaction was monitored at 340 nm. Data for A_{340nm} versus time were fitted to eq 1 to determine v_0, v_{lim}, and k'. This method assumes that the steady-state velocity measured immediately following dilution (v_0) reflects that fraction of enzyme initially present as E·nucl plus E·nucl·ald$_0$ ($f_{E\cdot nucl} + f_{E\cdot nucl\cdot ald}$ = ([E·nucl] + [E·nucl·ald]/[E·nucl]$_t$), whereas the E·adduct fraction ($f_{E\cdot adduct}$) only slowly becomes available for catalytic turnover. Because this is an approach to a new equilibrium level of E·adduct, k' determined by using eq 1 includes a contribution due to k'_f (see Appendix, eq 24). The k'_f component, calculated for [glycolaldehyde] = 5 mM by using the kinetic constants for E·NADP–ald formation (k'_f will largely be due to reaction of $NADP^+$ because [NADPH] ≫ [$(AP)ADP^+$]), was subtracted from k' to obtain k'_r.

To estimate the stoichiometry of E·adduct formation v_0 was compared with $v_{control}$, the initial velocity measured for an identical sample incubated without glycolaldehyde. Assuming as above that $v_0/v_{control}$ is equal to the sum $f_{E\cdot nucl} + f_{E\cdot nucl\cdot ald}$, then $f_{E\cdot adduct} = 1 - v_0/v_{control}$. From $f_{E\cdot adduct}$ we can determine a value for K'_{add} by using the expression derived in the preceding paper (Grimshaw et al., 1990):

$$f_{E\cdot adduct} = [E\cdot adduct_0]/[E\cdot nucl]_t = K'_{add}/(1 + K'_{add} + K_{lald}/[ald_0]) \quad (2)$$

Data Processing. The experimental data were fitted to the equations in the text by the least-squares method using the Fortran programs of Cleland (1979). Linear double-reciprocal plots were fitted to eq 3, and eq 4 was used when substrate inhibition was observed. Equations 5–7 describe intersecting

$$v_i = VA/(K_a + A) \quad (3)$$

$$v_i = VA/(K_a + A + A^2/K_{Ia}) \quad (4)$$

$$v_i = VAB/(K_bA + K_aB + K_{ia}K_b + AB) \quad (5)$$

$$v_i = VAB/[K_bA + K_aB + K_{ia}K_b + AB(1 + B/K_{Ib})] \quad (6)$$

$$v_i = VAB/[K_bA + (K_aB + K_{ia}K_b) \times (1 + B/K_{Ibs}) + AB(1 + B/K_{Ibi})] \quad (7)$$

$$v_i = VA/[K_a(1 + I/K_i) + A] \quad (8)$$

$$v_i = V/(1 + I/K_i) \quad (9)$$

initial velocity patterns; the latter two equations include terms in the denominator corresponding to uncompetitive (K_{Ib} in eq 6) and noncompetitive (K_{Ibs} and K_{Ibi} in eq 7 are the apparent slope and intercept inhibition constants) substrate inhibition by B, respectively. Equation 8 describes linear competitive inhibition by I versus A, and eq 9 describes a Dixon plot (Dixon, 1953) used for determination of the apparent K_i at fixed A. K_a and K_b are the Michaelis constants for A and B, respectively, K_{ia} and K_{Ia} are the apparent dissociation constant and substrate inhibition constants for A, respectively, and V is the maximum velocity. The kinetic nomenclature used is that of Cleland (1963a).

Results

Reaction of Glycolaldehyde with Adenine-Containing Nucleotides. Reaction of glycolaldehyde (90 mM) with ADP-ribose (50 μM) at 25 °C (50 mM sodium phosphate and 0.1 mM Na_2EDTA, pH 7.0) displayed a first-order increase ($t_{1/2} \approx 500$ s) in A_{272nm} in the difference spectrum (spectrum$_t$ − spectrum$_{t=0}$) (Figure 1). A similar reaction was observed for a series of adenine-containing nucleotides [adenosine, AMP, ADP, ATP, ADP-ribose, $NADP^+$, NADPH, $(AP)ADP^+$, and (AP)ADPH] but not with the nicotinamide mononucleotides NMN and NMNH nor with $N(Hx)DP^+$ and N(Hx)DPH, which have −OH in place of the 6-NH_2 moiety of adenine. ADP-ribose was chosen as an example because in that case the reaction with glycolaldehyde is not complicated by absorbance changes due to adduct formation (Grimshaw et al., 1990) or aldehyde-induced autoxidation (Wolf & Crabbe, 1985). The reaction can be described by the equation

$$\Delta A_{obs} = \Delta A_{max}[ald_0]_t/(K_{eq}^{-1} + [ald_0]_t) \quad (10)$$

where ΔA_{obs} and ΔA_{max} are the observed and maximum ΔA_{272nm}, respectively, $\Delta A_{max} = [nucl]_t\Delta\epsilon$ where $\Delta\epsilon = \epsilon_{product} - \epsilon_{nucl}$, $[nucl]_t$ is the total nucleotide concentration, $[ald_0]_t$ is the total concentration of the free aldehyde plus hydrate forms of glycolaldehyde, and $K_{eq} = [product]/[nucl][ald_0]_t$. (Since $[ald_0]_t \gg [nucl]_t$, $[ald_0]_t$ remains essentially constant during the reaction). Data for ΔA_{obs} versus $[ald_0]_t$ (30–90 mM) were fitted to eq 3, which has the same form as eq 10, and gave $\Delta\epsilon_{272nm} \approx 10\,000$ M^{-1} cm^{-1} and $K_{eq} = 0.8$ M^{-1}.

Substrate and Product Inhibition Patterns. Substrate inhibition of the initial velocity was noncompetitive versus NADPH ($K_{Ibs} \approx 10K_{Ibi}$ determined from fits to eq 7) when the substrate (b = glycolaldehyde) was preincubated with NADPH before enzyme was added to start the reaction (not shown). When glycolaldehyde was added last to start the reaction, K_{Ibs} was no longer statistically significant and the data were fitted to eq 6. The competitive inhibition component was also absent when N(Hx)DPH was used (Figure 2), regardless of the order of substrate addition. Values of the kinetic parameters determined from fits to eq 6 for reduction of glycolaldehyde with NADPH, (AP)ADPH, and N(Hx)DPH at pH 7.0 (MOPSE buffer) and 15 °C are listed in Table I. Similar results (i.e., uncompetitive substrate inhibition versus NADPH) were obtained for *p*-nitrobenzaldehyde at pH 7.0 and 25 °C, with $K_b = 0.02$ mM and $K_{Ib} = 5.0$ mM (not shown). Kinetic constants determined for both the forward and reverse ALR2-catalyzed reactions at pH 8.0 (MOPSE buffer) and 15 °C are listed in Table II. Initial velocities for

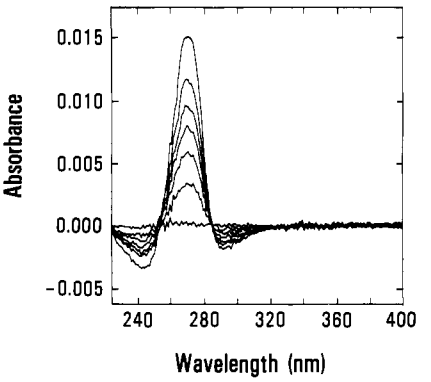

FIGURE 1: Spectrophotometric demonstration of nonenzymic reaction of glycolaldehyde and ADP-ribose. Reaction mixture contained 50 μM ADP-ribose or 90 mM glycolaldehyde in 50 mM sodium phosphate and 0.1 mM Na_2EDTA buffer (pH 7.0, 25 °C) in separate compartments of dual tandem cells (total path length = 0.9 cm). Spectra shown are difference spectra (sample − reference)$_t$, corrected for the initial spectrum (sample − reference)$_{t=0}$, measured at t = 0.07, 3, 6, 9, 12, 18, and 30 min after the reaction was started by mixing the contents of the sample cell.

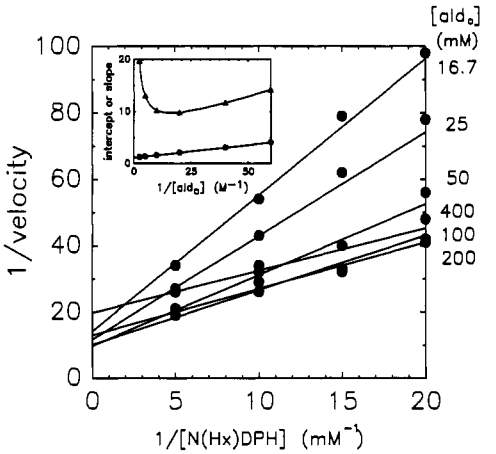

FIGURE 2: Initial velocity pattern for glycolaldehyde and N(Hx)DPH. Initial velocity was measured as ΔA_{340}/min at 25 °C in MOPSE buffer containing 0.50 μM ALR2 (added last) and the indicated concentration of N(Hx)DPH and glycolaldehyde (ald_0). The points are the experimental values, and the curve was calculated from a fit to eq 6 with $V = 0.19 \pm 0.03$ A_{340}/min, $K_a = 0.22 \pm 0.05$ mM, $K_b = 24 \pm 12$ mM, $K_{ia} = 0.35 \pm 0.15$ mM, and $K_{Ib} = 150 \pm 30$ mM [A = N(Hx)DPH, B = glycolaldehyde]. The inset shows a replot of the slopes (●) and intercepts (▲) derived from the primary plot versus $1/[ald_0]$; the line (●) and curve (▲) are calculated from fits to eqs 3 and 4, respectively.

Table I: Kinetic Constants for Alternate Nucleotide Substrates[a]

constant	nucleotide		
	NADPH[b]	(AP)ADPH[b]	N(Hx)DPH[c]
$V_{glycolaldehyde}/E_t$ (s^{-1})	0.59 ± 0.01	0.60 ± 0.06	0.63 ± 0.03
K_{nuclH} (μM)	≤0.2	≤0.2	150 ± 30
$K_{glycolaldehyde}$ (mM)	4.0 ● 1.0	25 ± 4	5.9 ± 1.9
K_{inuclH} (μM)	0.046 ± 0.015[d]	0.22 ± 0.04[d]	680 ± 230
K_{Iald} (mM)	35 ± 5	166 ± 20	160 ± 40

[a] MOPSE buffer, 15 °C, with glycolaldehyde added last to start the reaction; values obtained from fits to eq 6; nuclH is reduced nucleotide. [b] Initial velocity measured as $\Delta_{365}F_{480}$/time with 0.2 μM ALR2. [c] Initial velocity measured as ΔA_{340}/time with 0.5 μM ALR2. [d] Values determined by fluorescence titration (Grimshaw et al., 1990).

Table II: Kinetic Constants at pH 8.0[a]

$V_{glycolaldehyde}/E_t$[b] (s^{-1})	0.18 ± 0.01
$K_{glycolaldehyde}$ (mM)	1.0 ± 0.1
$V_{ethyleneglycol}/E_t$[c] (s^{-1})	0.020 ± 0.001
K_{NADP} (μM)	0.10 ± 0.05
K_{iNADP} (μM)	0.10 ± 0.04
$K_{ethyleneglycol}$ (M)	4.0 ± 0.3

[a] 50 mM Mops, 0.1 mM Na_2EDTA, 15 °C. [b] Initial velocity measured as ΔA_{340}/time with 100 μM NADPH and 0.5 μM ALR2. [c] Initial velocity measured as $\Delta_{365}F_{480}$/time with 0.1 μM ALR2.

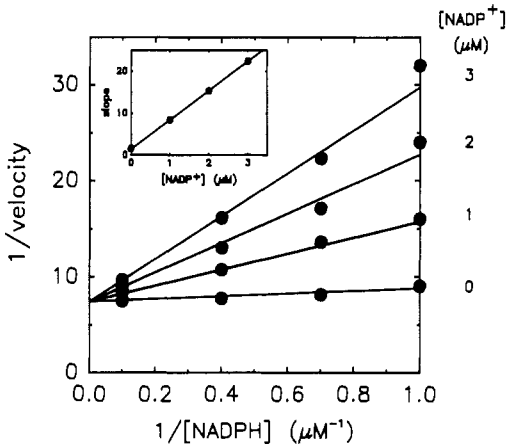

FIGURE 3: Competitive product inhibition by $NADP^+$ versus NADPH. Initial velocity was measured by fluorescence ($_{340}F_{460}$; slits 2 nm excitation, 10 nm emission) at 15 °C in MOPSE buffer containing 0.10 μM ALR2 and 5 mM glycolaldehyde. The points are the experimental values, and the lines are calculated from a fit to eq 8 with $V = 0.136 \pm 0.002$, $K_a = 0.19 \pm 0.03$ μM, and $K_i = 0.20 \pm 0.03$ μM (A = NADPH, I = $NADP^+$). The inset shows a replot of the slopes derived from the primary plot versus 1/[NADPH]; the points are from fits to eq 3 of data for each [$NADP^+$] level and the line is calculated by using eq 8.

oxidation of ethylene glycol with $NADP^+$ (full pattern) were fitted to eq 5, and those for reduction of glycolaldehyde at saturating NADPH (100 μM) were fitted to eq 4.

Product inhibition by $NADP^+$ was competitive versus NADPH (Figure 3). When fitted to eq 8, the data gave $K_{iNADP} = 0.20 \pm 0.03$ μM and app $K_{NADPH} = 0.19 \pm 0.03$ μM ($[ald_0] = 5$ mM). However, because the measured K_i value was comparable to $[ALR2]_t = 0.10$ μM, the data were also analyzed by using the equation

$$v_i = -(VA_tB_t/2E_t)[\Sigma + (I_t - E_t)/D] + \tfrac{1}{2}\{[[\Sigma + (I_t - E_t)/D]^2 + (4\Sigma V_t^2A_t^2B_t^2/DE_t)]^{1/2}\} \quad (11)$$

which describes reversible tight-binding inhibition by $NADP^+$ versus NADPH (Williams & Morrison, 1979), where $\Sigma = K_{is}/K_{ia}K_b$; $D = K_{ia}K_b + K_{bA} + K_aB + AB$; $K_{is} = K_{iNADP}$; A_t, B_t, I_t, and E_t are the total concentrations of NADPH, glycolaldehyde, $NADP^+$, and ALR2 respectively; and the remaining constants are as defined in eq 5. To fit the data to eq 11, V, E_t, B_t, and K_b were fixed and K_{is}, K_a, and K_{ia} were optimized by nonlinear least-squares analysis (Dixon, 1988) with v_i as the dependent variable. Examination of the least-squares surface (Cleland, 1979) revealed that K_{is} and K_{ia} were highly correlated ($K_{is} \approx 2K_{ia}$), yet the K_a value ranged from 0 to 0.2 μM with little change in the residual sum of squares (SS). The fit of eq 11 did, however, give K_{is} (0.15 ± 0.02 μM) and K_{ia} (0.08 ± 0.01 μM) values much closer to those determined by fluorescence titration (Grimshaw et al., 1990) with an SS value (9.0×10^{-5}) comparable to that seen in the fit to eq 8 (SS = 7.0×10^{-5}).

Estimation of E·Adduct Decomposition Rate and Stoichiometry. A representative product versus time curve for

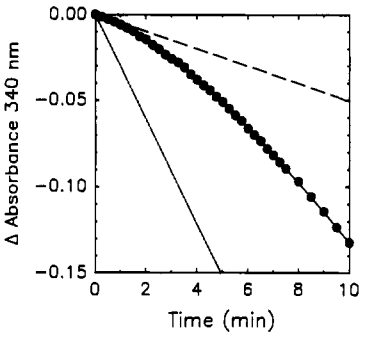

FIGURE 4: Direct measurement of E·adduct decomposition from time course for recovery of ALR2 activity. Final concentrations in the reaction mixture were 1.0 μM (AP)ADP^+, 160 μM NADPH, 5 mM glycolaldehyde, and 0.31 μM ALR2 in MOPSE buffer, 15 °C. The assay was started by diluting an aliquot of ALR2 (40 μL), consisting of the equilibrium distribution of E·(AP)ADP, E·(AP)ADP·ald_0, and E·$adduct_0$, into a final volume of 1.0 mL. The points are the actual A_{340} values, and the curve is from a fit to eq 1 with $v_0 = 0.0051 \pm 0.0003$ A_{340}/min, $v_{lim} = 0.020 \pm 0.001$ A_{340}/min, and $k' = 0.0047 \pm 0.0002$ s^{-1}. Lines are also shown for v_0 (- - -) and $v_{control} = 0.031$ A_{340}/min (····).

Table III: Comparison of Kinetic Parameters for Adduct Formation[a]

parameter	method	nucleotide: NADPH	nucleotide: (AP)ADPH
$K_{Iald}(1 + k'_7/k'_5)$ (mM)	*b*	35 ± 5	166 ± 20
	c	34 ± 4	182 ± 15
	d	29 ± 6	250 ± 150
$K_{Iald}(1 + k'_7/k'_5)/(1 + K'_{add})$ (mM)	*e*	6.7 ± 0.6	6.5 ± 0.5
K_{Iald} (mM)	*f*	25 ± 1	140 ± 30
$K_{Iald}/(1 + K'_{add})$ (mM)	*f*	4.8 ● 0.7	4.9 ± 1.0
K'_{add}	*g*	4.1 ± 0.6	24 ± 4
	h	≥2.1	≥20
	f	4.4 ± 0.6	30 ± 8
k'_r (s^{-1})	*h*	$(7.8 \pm 2.1) \times 10^{-3}$	$(1.5 \pm 0.2) \times 10^{-3}$
	i	$(6.7 \pm 0.7) \times 10^{-3}$	$(1.3 \pm 0.3) \times 10^{-3}$
	f	$(4.7 \pm 0.3) \times 10^{-3}$	$(1.0 \pm 0.1) \times 10^{-3}$
k'_f (M^{-1} s^{-1})	*d*	$(7.9 \pm 0.9) \times 10^5$	$(2.7 \pm 1.2) \times 10^5$
	f	$(6.0 \pm 1.1) \times 10^5$	$(1.5 \pm 0.1) \times 10^5$

[a] MOPSE buffer, 15 °C. [b] K_{Ib} value determined from fit of initial velocity pattern to eq 6. [c] App K_i from $1/v_o$ versus [ald_o] (eq 9). [d] Value obtained from variation of $1/(k'_{app} - k'_r)$ versus $1/[ald_o]$ (eq 25). [e] App K_i from $1/v_{lim}$ versus [ald_o] (eq 9). [f] Average values determined from data for E·adduct formation in the absence of glycolaldehyde turnover (Grimshaw et al., 1990). [g] Calculated from the ratio of app K_i values for $1/v_o$ and $1/v_{lim}$ (eq. 21). [h] Calculated by using eq 2 and $f_{E\text{·adduct}}$ value obtained from the time course for recovery of ALR2 activity due to breakdown of E·adduct (Figure 4). [i] Calculated as $k'_{app}v_{lim}/v_o$ (eq 26).

recovery of ALR2 activity following decomposition of E·(AP)ADP–ald is shown in Figure 4. The k'_{app} value determined from a fit to eq 1 [$(4.7 \pm 0.2) \times 10^{-3}$ s^{-1}] was corrected for the contribution of k'_f (3.2×10^{-3} s^{-1}; see Appendix, eq 24) to give $k'_r = (1.5 \pm 0.2) \times 10^{-3}$ s^{-1}. A similar time course determined for E·NADP–ald decomposition gave $k'_r = (7.8 \pm 2.1) \times 10^{-3}$ s^{-1}. The observed $v_0/v_{control}$ ratios and (in parentheses) the calculated $f_{E\text{·adduct}}$ values were 0.42 (0.58) for E·NADP–ald and 0.16 (0.84) for E·(AP)ADP–ald. These $f_{E\text{·adduct}}$ values were analyzed by using eq 2 to yield K'_{add} estimates of ≥2.1 and ≥20, respectively. This method appeared to underestimate K'_{add} and overestimate k'_r relative to the results obtained by other methods (see Table III). For (AP)ADP–ald, the discrepancy was less, presumably because the 5-fold slower k'_r allowed more accurate measurement of the initial portion of the time course for adduct breakdown.

Nonlinear Product versus Time Plots for Aldehyde Reduction. In addition to uncompetitive substrate inhibition (versus NADPH) of the *initial* steady-state rate (v_0), glycolaldehyde showed a time-dependent decay to a limiting steady-state rate (v_{lim}) (Figure 5). Similar results were ob-

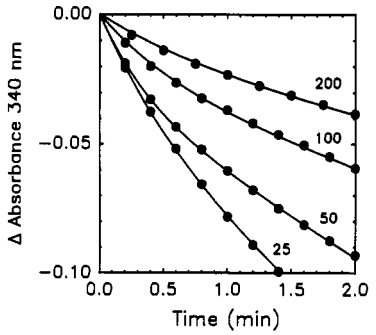

FIGURE 5: Product versus time curves for ALR2-catalyzed reduction of glycolaldehyde with NADPH. Assays were conducted at 15 °C in MOPSE buffer containing 160 μM NADPH and 0.625 μM ALR2. The indicated concentration of glycolaldehyde was added last to start the reaction. Data for the first 2 min of the experimental reaction time courses are shown; the curves are calculated by using v_0, v_{lim}, and k' determined from fits to eq 1.

Scheme I

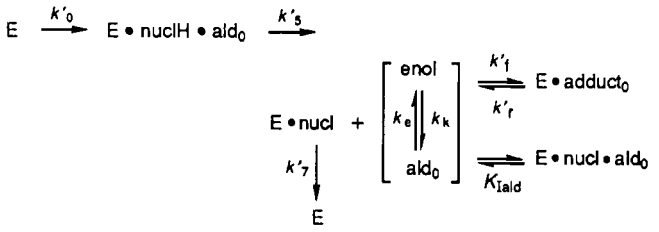

tained with (AP)ADPH (not shown). Control experiments involving preincubation of ALR2 with various combinations of reaction components (buffer, NADPH, glycolaldehyde) showed that this transient did not result from a hysteretic transition (Neet & Ainslie, 1980) or inactivation of the enzyme, from simple product inhibition by $NADP^+$ [or (AP)-ADP^+], or from the approach to equilibrium. However, when ALR2 was first preincubated with glycolaldehyde and $NADP^+$ [or (AP)ADP^+] for sufficient time (45 min) to allow adduct formation at the active site to reach equilibrium (Grimshaw et al., 1990), the reaction time course showed an *initial* steady-state rate (equal to v_{lim} measured without preincubation) that gradually *increased* to a final steady-state rate equal to v_0 measured for a control mixture preincubated without glycolaldehyde (Figure 4; see above). In contrast, *p*-nitrobenzaldehyde showed uncompetitive substrate inhibition of v_0 but did not show the decay of v_0 to v_{lim}.

Kinetic Analysis of Product versus Time Plots for Glycolaldehyde Turnover. Reaction time courses were analyzed by using a modification (Scheme I) of the mechanism for ALR2-mediated E·adduct formation presented previously (Grimshaw et al., 1990), where enol is glycolaldehyde enol, nucl is oxidized nucleotide (e.g., $NADP^+$), nuclH is reduced nucleotide (e.g., NADPH), and ald_0 and $adduct_0$ are the sum of free aldehyde plus hydrate forms of glycolaldehyde and adduct, respectively. Glycolaldehyde turnover requires that we include the following net rate constants (Cleland, 1975): k'_0 for conversion of (E + nuclH + ald_0) to E·nuclH·ald_0, k'_5 for the catalytic step (E·nuclH·ald_0 → E·nucl·alcohol) and release of alcohol product (ethylene glycol), and k'_7 for release of nucl from E·nucl. The other kinetic constants have been defined previously (Grimshaw et al., 1990). Of the two inhibitory complexes, E·nucl·ald_0 and E·$adduct_0$, the former is responsible for the inhibition of v_0, and both complexes contribute to the inhibition of v_{lim}.

According to the rate equation that describes Scheme I (see Appendix), a Dixon plot of E_t/v_0 or E_t/v_{lim} versus I, where $I = [ald_0]$, should display a linear increase with an apparent

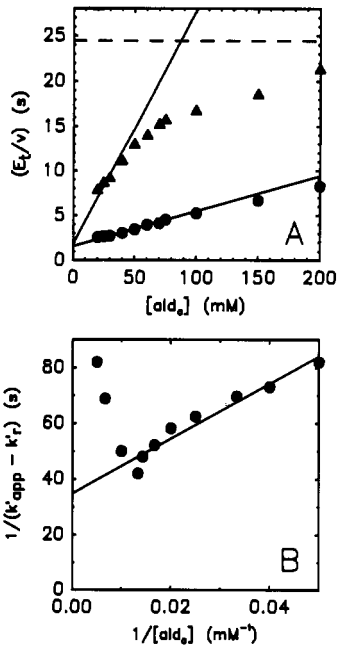

FIGURE 6: Replot of kinetic parameters derived by analysis of product versus time curves for glycolaldehyde reduction. (A) Replot versus $[ald_0]$ of E_t/v_0 and E_t/v_{lim} determined from fits to eq 1 of the product versus time curves in Figure 5. The points are the least-squares estimates; the lines for v_0/E_t (●) and v_{lim}/E_t (▲) are calculated from fits to eq 9 with app K_i values of 34 ■ 4 mM and 6.7 ± 0.6 mM (for $[ald_0] \leq 60$ mM), respectively, and 0.57 ± 0.08 s^{-1} as the app $V = V/E_t$. The minimum v_{lim}/E_t value ($v_{inhib}/E_t = 0.041$ s^{-1}) determined from a fit to eq 3 of the quantity $E_t(1/v_{lim} - 1/V)$ versus $[ald_0]$ is also shown (---). (B) Double-reciprocal plot of $1/(k'_{app} - k'_r)$ versus $1/[ald_0]$ for k'_{app} values determined from the reaction time courses in Figure 5 and corrected by using $k'_r = 0.0064$ s^{-1}. The line is a least-squares fit to eq 3 with 29 ± 6 mM as the apparent $K_a = K_{Iald}(1 + k'_7/k'_5)$ and 0.028 ± 0.003 s^{-1} as the apparent $V = k'_f K_{enol} K_{Iald}$ (eq 24).

K_i equal to $K_{Iald}(1 + k'_7/k'_5)$ for E_t/v_0 and equal to $K_{Iald}(1 + k'_7/k'_5)/(1 + K'_{add})$ for E_t/v_{lim}. Product versus time data for ALR2-catalyzed reduction of glycolaldehyde with NADPH at 15 °C (Figure 5) were fitted to eq 1, and the resultant values of E_t/v_0 and E_t/v_{lim} were plotted versus $[ald_0]$ (Figure 6A). As shown, E_t/v_0 displayed the predicted linear increase with an apparent K_i (34 ± 4 mM) determined from a fit to eq 9 that was similar to K_{Ib} (35 ± 5 mM) determined from the full initial velocity pattern (Table I). A linear increase was also observed for E_t/v_{lim} (for $[ald_0] \leq 60$ mM) with an apparent $K_i = 6.7 \pm 0.6$ mM. For (AP)ADPH, the predicted linear variation with increasing $[ald_0]$ was again seen for both E_t/v_0 and E_t/v_{lim} (for $[ald_0] \leq 150$ mM) (not shown), and the apparent K_i values, along with the K'_{add} values calculated from their ratio (see Appendix, eq 21), are listed in Table III. Also shown for comparison are the values of K_{Iald}, $K_{Iald}/(1 + K'_{add})$, and K'_{add} determined in the preceding paper (Grimshaw et al., 1990) for E·$adduct_0$ formation in the absence of glycolaldehyde turnover.

Scheme I further predicts that the quantity $k'_{app} - k'_r$, where k'_{app} is the apparent first-order rate constant for transition from v_0 to v_{lim}, will display saturation kinetics as $[ald_0]$ is increased above an apparent half-saturation constant equal to $K_{Iald}(1 + k'_7/k'_5)$ and will approach a maximum of $k'_f K_{enol} K_{Iald}$ (see Appendix, eq 24). Figure 6B shows a double-reciprocal plot of $1/(k'_{app} - k'_r)$ versus $1/[ald_0]$ for the k'_{app} values obtained from fits to eq 1 of the data shown in Figure 5. As predicted, saturation kinetics were observed for $[ald_0] \leq 60$ mM, the same concentration range over which $1/v_{lim}$ displayed a linear dependence on $[ald_0]$. Similar results were obtained for

(AP)ADPH (for $[ald_0] \leq 150$ mM), although the intercept value, and thus k'_f, was not well determined (not shown). The $K_{Iald}(1 + k'_7/k'_5)$ and k'_f values obtained from fits to eq 3 of data from the linear asymptote region of these double-reciprocal plots are listed in Table III.

The k'_r values used to calculate $k'_{app} - k'_r$ were determined in three ways: (1) as the average value of $k'_{app}v_{lim}/v_0$ (see Appendix, eq 26), calculated by using data from the linear concentration range (see above); (2) from the time course for recovery of ALR2 activity (see Figure 4); and (3) by direct measurement of E·adduct breakdown (Grimshaw et al., 1990). The k'_r values estimated by these three methods were in good agreement (see Table III).

By contrast to the steady decline predicted for v_{lim}, inspection of Figure 6A clearly shows only partial inhibition. The minimum rates (v_{inhib}/E_t), determined by fitting the quantity $E_t(1/v_{lim} - 1/V)$ as a function of $[ald_0]$ to eq 3, were $(4.1 \pm 0.6) \times 10^{-2}$ s^{-1} for NADPH and $(6.6 \pm 0.7) \times 10^{-3}$ s^{-1} for (AP)ADPH.

Discussion

Substrate Inhibition by Glycolaldehyde. Bovine kidney ALR2 displays substrate inhibition by most aldehyde substrates (Grimshaw et al., 1989). As shown in Figure 2, the inhibition by glycolaldehyde was uncompetitive versus N(Hx)DPH, which for an ordered kinetic mechanism requires that glycolaldehyde bind either to the central complexes or to E·nucl (Cleland, 1963b). With NADPH, however, the inhibition was noncompetitive when the aldehyde was allowed to react with NADPH prior to the enzyme assay. On the basis of model studies of the reaction of aldehydes (McGhee & von Hippel, 1975; Fraenkel-Conrat & Singer, 1988) and epoxides (Windmuller & Kaplan, 1961) with the adenine ring, we have tentatively identified the product of this nonenzymic reaction, characterized by an absorbance peak at 272 nm in the difference spectrum ($\Delta\epsilon_{272nm} \approx 10000$ M^{-1} cm^{-1}) (Figure 1), as β-nicotinamide N_6-(1,2-dihydroxyethyl)adenine dinucleotide phosphate (reduced form), the carbinolamine derived by reaction of glycolaldehyde with the 6-NH_2 group of adenine.

Given the K_{eq} value for this reaction (0.8 M^{-1}), simple depletion of NADPH can account for about 40% of the slope inhibition component. Oxidation of NADPH to $NADP^+$ via nonenzymic autooxidation of glycolaldehyde [e.g., see Wolff and Crabbe (1985)] may account for the remainder, although Chelex-100 treatment of all solutions should have minimized this side reaction. Since ALR2 appears to be sensitive to changes in the adenine moiety (Table I), the carbinolamine product is not expected to compete effectively with NADPH. Fortunately, the reaction is slow ($t_{1/2} \approx 500$ s), and thus adding glycolaldehyde last to start the enzyme assay eliminates the competitive substrate inhibition component seen with NADPH.

The extent to which this type of nonenzymic modification of NAD(P)H might affect the reaction kinetics of other aldehyde reductases is not known. Enzymes that are sensitive to changes in the adenine moiety, including glyceraldehyde-3-phosphate dehydrogenase and yeast alcohol dehydrogenase, should be more affected than less selective enzymes, such as lactate dehydrogenase or horse liver alcohol dehydrogenase (Suhadolnik, et al., 1977). At a minimum, our results suggest that reactive carbonyl compounds should not be incubated with adenine nucleotides for prolonged periods of time prior to starting an enzyme assay.

Nonlinear Time Courses for Aldehyde Reduction. In addition to inhibition of the *initial* steady-state velocity described above, glycolaldehyde displayed a time-dependent onset of further inhibition (Figure 5). *p*-Nitrobenzaldehyde, which does not contain an enolizable α-proton, also displayed substrate inhibition of the initial velocity yet did not show any decay to a lower, *limiting* steady-state velocity. These observations, coupled with preliminary spectroscopic evidence of NADP–glyceraldehyde adduct formation, lead us to suggest (McKercher et al., 1985; Grimshaw, 1986) that substrate inhibition of ALR2 might occur via a mechanism similar to that described for pyruvate inhibition of lactate dehydrogenase (Gutfreund et al., 1968; Burgner et al., 1978).

Scheme II

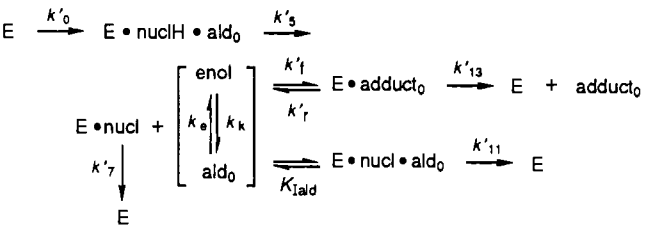

The experiments reported here and in the preceding paper (Grimshaw et al., 1990) have confirmed this mechanism as the basis for the nonlinear product versus time curves for ALR2-catalyzed reduction of glycolaldehyde. Thus, as detailed under Results, the variation of the observable quantities (v_0, v_{lim}, and k'_{app}) with increasing glycolaldehyde concentration (up to a certain limit) can be predicted from the equations derived to describe Scheme I. (Modification of Scheme I to accommodate partial substrate inhibition of v_{lim} is discussed in the following section.) In addition, as shown in Table III, the values of k'_f, k'_r, and K'_{add} derived from these data are in excellent agreement with the values obtained from analysis of ALR2-mediated adduct formation in the absence of glycolaldehyde turnover (Grimshaw et al., 1990).

Adduct formation has practical consequences for kinetic studies of ALR2. In particular, for short-chain aldoses where the acyclic free aldehyde and enol forms are present in significant amounts, the onset of inhibition can be quite rapid. For ALR2-catalyzed reduction of glyceraldehyde at 25 °C (0.1 M sodium phosphate buffer, pH 7.0), $t_{1/2} \approx 10$ s for the decay in v_0 due to adduct formation (Mathur et al., 1985; Grimshaw, 1986, 1987). Furthermore, because the rate of decay varies as a function of $[ald_0]$ (Figure 6B), the tendency to *underestimate* v_i is greatest at the high substrate concentrations where v_i otherwise begins to deviate toward *higher* rates when a mixture of activated and unactivated ALR2 is analyzed (Grimshaw et al., 1989). Thus, one could obtain a linear double-reciprocal plot of $(1/v_i)_{obsd}$ versus $1/[ald_0]$, when in fact the plot of $(1/v_i)_{true}$ versus $1/[ald_0]$ would show the negative cooperativity characteristic of a partially activated enzyme sample. These results may explain why activation of ALR2 has not been more generally recognized. We suggest that either nonenolizable substrates (e.g., substituted benzaldehydes) or long-chain aldoses be used in future kinetic studies to avoid the complicating effects of adduct formation.

Rationale for Partial Substrate Inhibition. According to Scheme I, v_{lim} should approach zero as $[ald_0] \rightarrow \infty$, but this is clearly not the case for either NADPH (Figure 6A) or (AP)ADPH (not shown). Thus, there must be an alternate reaction pathway at high $[ald_0]$ as shown in the modified mechanism in Scheme II, which includes net rate constants for release of adduct from E·$adduct_0$ (k'_{13}) and for conversion of E·nucl·ald_0 back to free E (k'_{11}). The value of k'_r for E·NADP–ald_0 measured directly (0.005–0.008 s^{-1}; see Table III) sets an upper limit on the value of k'_{13}. Since v_{inhib}/E_t for NADPH (0.041 s^{-1}) was about 6-fold faster than this value,[2] E·$adduct_0$ release cannot account for the residual re-

action flux. Similarly, v_{inhib}/E_t for (AP)ADPH was about 5-fold faster than k'_r measured for E·(AP)ADP–ald_0.

Next we consider the rate constant (k'_{11}) for conversion of the ternary E·nucl·ald_0 complex back to E. At the [ald_0] levels where v_{lim} approaches v_{inhib} [i.e., for [ald_0] $\gg K_{Iald}(1 + k'_7/k'_5)$], the fraction of [E·nucl]$_t$ present as E·nucl·ald_0 will be equal to $1/(1 + K'_{add})$ (see Appendix, eq 18). Given $K'_{add} \approx$ 4.4 for E·NADP–ald_0 (Table III), we calculate that k'_{11} must be at least 0.22 ± 0.06 s^{-1} in order for the product ($k'_{11}f_{E\text{-}nucl\text{-}ald}$) to equal v_{inhib}/E_t. If that were the case, then v_0/E_t must also approach k'_{11} at high [ald_0] levels because under those conditions virtually all the enzyme will be present as E·nucl·ald_0. As shown in Figure 6A, the lowest v_0/E_t value determined for NADPH (0.13 s^{-1} at [ald_0] = 200 mM) was within range of the predicted k'_{11} value, given the uncertainty in v_0/E_t at these high [ald_0] levels. For (AP)ADPH, the lowest v_0/E_t value (0.17 s^{-1} at [ald_0] = 400 mM) was also within range of the predicted minimum k'_{11} value (0.19 ± 0.05 s^{-1}). These data, therefore, cannot exclude the possibility of an alternate pathway in which nucl is released before ald_0.

Finally, an increase in the net rate constant for nucl release (k'_7) to a faster rate (k''_7) at high [ald_0], possibly due to chemial modification of the active-site lysine 262 (Schade et al., 1987; Morjana et al., 1989), could also explain the partial inhibition. Activation of liver alcohol dehydrogenase via an increase in the off rate for NAD^+ has been shown to result from chemical modification of a single active-site lysine by pyridoxal (Sogin & Plapp, 1975), and a similar effect may be involved in the activation of human muscle ALR2 by pyridoxal phosphate (Morjana et al., 1989). In that case, E_t/v_{lim} should continue to increase above the plateau seen in Figure 6A, albeit with a lower slope, and our data cannot rule out this possibility either.

Kinetic Mechanism. Previously, we proposed a mechanism (eq 12) for the ALR2 reaction that involved isomerization of the free enzyme (Grimshaw et al., 1989). The assignment

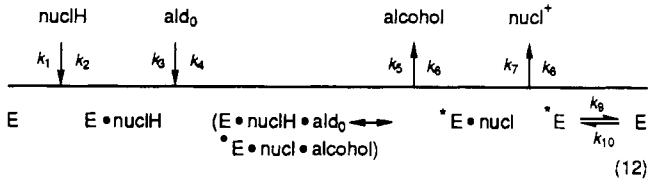

(12)

of this step as the rate-limiting one for the unactivated enzyme form was based on the observation of similar $V_{aldehyde}/E_t$ values for a range of aldehyde substrates. According to this mechanism, $NADP^+$ should display noncompetitive product inhibition versus NADPH. However, as shown in Figure 3, the pattern is clearly competitive, and a closer look at these data suggests why the previous analysis was incorrect.

As we have shown (Grimshaw et al., 1990), ALR2 binds both the reduced and oxidized nucleotide cofactors very tightly (K_{dNADPH} = 46 ± 15 nM; K_{dNADP} = 80 ± 30 nM). Because the turnover number is also low ($V_{glycolaldehyde}/E_t$ = 0.59 s^{-1}), the concentration of enzyme ($[E]_t$ = 0.10 μM) was found to be comparable to the K_{NADPH} (0.19 ± 0.03 μM) and K_{iNADP} (0.20 ± 0.03 μM) values determined by fitting the data in Figure 3 to eq 8. Yet, under those conditions the assumption inherent in the use of eq 8 (i.e., $[E]_t \ll [NADPH]_t$ and $[NADP^+]_t$) is no longer valid, and correction must be made for the depletion of free NADPH and $NADP^+$ by binding to the enzyme (Williams & Morrison, 1979). Accordingly, when the data were analyzed by using an equation that describes competitive tight-binding inhibition for $NADP^+$ versus NADPH (eq 11), the resultant fit gave values for K_{iNADPH} (0.08 ± 0.01 μM) and K_{iNADP} (0.15 ± 0.02 μM) that were much closer to those determined by fluorescence titration (Grimshaw et al., 1990).

The apparent K_{NADPH} and K_{iNADP} values determined by using eq 8 will be limited by the $[E]_t$ level used in the assay if no correction is made for tight binding, and this effect should be greater for the unactivated relative to the activated enzyme, since assays of the former require a higher $[E]_t$ level to offset the 14-fold lower turnover number. Our earlier assignment of the isomerization step to the free enzyme was based in part on a 5-fold lower K_{iNADPH} value and little change in K_{NADPH} following enzyme activation (Grimshaw et al., 1989). If, however, the apparent values determined for the unactivated enzyme were too high, because of the tight-binding effect discussed above, that would explain the observed kinetics *without* invoking isomerization of the free enzyme.

What then is the mechanistic basis for the similar $V_{aldehyde}/E_t$ values seen for the three nucleotide substrates with glycolaldehyde (Table I) and for a range of aldehyde substrates with NADPH (Grimshaw et al., 1989)? The kinetic results at pH 8.0 (Table III) suggest isomerization of E·nucl as the answer. Thus, calculation of k_7 for the mechanism shown in eq 12 by using the expression

$$k_7 = (V_{ethyleneglycol}/K_{NADP})K_{iNADP}$$

yields a value of 0.02 s^{-1} (range 0.01–0.06 s^{-1}). But the *overall* rate of reaction in this direction ($V_{glycolaldehyde}/E_t$) is 0.18 s^{-1} at pH 8.0, and k_7 must be at least this large. If, however, we assume a mechanism in which E·nucl, rather than E, undergoes isomerization, as in eq 13, then the above combination of kinetic constants is no longer equal to k_7 but instead

$$k_7k_9k_{10}/(k_7 + k_{10})(k_9 + k_{10})$$

which *can* have a value less than $V_{glycolaldehyde}/E_t$. The kinetic results at pH 8.0 thus support the mechanism shown as eq 13.

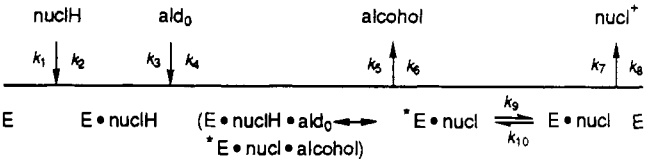

(13)

Two possible cases can be considered for eq 13, where the expression for the net rate constant k'_7 is

$$k_7k_9/(k_7 + k_{10})$$

If nucleotide release is much faster than the reverse isomerization step (i.e., $k_7 \gg k_{10}$), then $k'_7 = k_9$, and the only requirement for a constant $V_{glycolaldehyde}/E_t$ value for the three nucleotides is that k_9 be independent of the nucleotide used. Alternatively, if $k_7 \ll k_{10}$, then $k'_7 = k_7(k_9/k_{10})$ and k'_7 represents a rapid equilibrium isomerization step followed by a relatively slower off rate. Unfortunately, the present data do not allow us to distinguish between these two possibilities. However, we do know from the comparison of K_{Iald} and $K_{Iald}(1 + k'_7/k'_5)$ at pH 7 (see Table III) that $k'_7/k'_5 \leq 0.40$ for either NADPH or (AP)ADPH. Hence, because $V_{glycolaldehyde}/E_t = 1/(1/k'_5 + 1/k'_7)$, k'_7 must be at least 60% rate-determining at pH 7, or 0.6 $s^{-1} \leq k'_7 \leq$ 1.0 s^{-1}. In other words, at a saturating level of glycolaldehyde, at least 60% of $[E]_t$ will be present as [E·nucl + *E·nucl] in the steady state. In either case, the mechanism in eq 13 is still consistent with our earlier

[2] In the preceding paper (Grimshaw et al., 1990), we argue that the rate constant for NADP–ald_0 dissociation ($k_{off} \approx 4 \times 10^{-6}$ s^{-1}) is actually 1000-fold slower than k'_r.

proposal that the primary effect of enzyme activation is on an isomerization step, except that now it is isomerization of E·nucl rather than the unliganded enzyme. Thus, if k_9 is increased following enzyme activation, $V_{aldehyde}/E_t$ will increase and K_{inucl}, $V/K_{nuclH}E_t$, and $V/K_{aldehyde}E_t$ will not be affected. $V_{alcohol}/E_t$ and $V/K_{nucl}E_t$ must also be affected if k_{10} changes along with k_9, and K_{inucl} will increase unless k_{10} increases more than k_9. The latter predictions remain to be tested with the unactivated enzyme form.

ACKNOWLEDGMENTS

We thank Ms. Guiti Jahangiri for purification of bovine kidney aldose reductase and Ms. Sue Burke for assistance with the manuscript preparation.

APPENDIX

Analysis of Nonlinear Reaction Time Courses of Glycolaldehyde Reduction. According to Scheme I, the observed rate of glycolaldehyde reduction will decrease with time from an *initial* steady-state velocity (v_0) to a *limiting* steady-state velocity (v_{lim}). For v_0, we assume that no E·adduct has formed and inhibition is due solely to reversible formation of the E·nucl·ald dead-end complex. For v_{lim}, the steady-state level of E·nucl is assumed to be in rapid equilibrium with E·adduct and E·nucl·ald, with inhibition resulting from both of the latter complexes. k'_0 will not contribute to the observed rate because both nuclH and ald_0 are saturating. Given these assumptions, the steady-state rate for Scheme I is given by

$$v_i = E_t/(1/k'_5 + 1/k'_7 f_{E\cdot nucl}) \quad (14)$$

Substituting for $f^0_{E\cdot nucl}$, the *initial* fraction of $[E\cdot nucl]_t = ([E\cdot nucl] + [E\cdot nucl\cdot ald_0] + [E\cdot adduct_0])$ present as E·nucl

$$f^0_{E\cdot nucl} = [E\cdot nucl]_0/[E\cdot nucl]_t = 1/(1 + [ald_0]/K_{Iald}) \quad (15)$$

and using $V/E_t = k'_5k'_7/(k'_5 + k'_7)$, we have for v_0/E_t

$$v_0/E_t = (V/E_t)\{1 + [ald_0]/K_{Iald}(1 + k'_7/k'_5)\} \quad (16)$$

Equation 16 has the same form as eq 9:

$$v_i = V/(1 + I/K_i) \quad (9)$$

with $I = [ald_0]$ and $K_i = K_{Iald}(1 + k'_7/k'_5)$. The double-reciprocal form of eq 16

$$E_t/v_0 = E_t/V + [ald_0]E_t/\{V\cdot K_{Iald}(1 + k'_7/k'_5)\} \quad (17)$$

is better suited to graphical analysis, since the ordinate intercept (E_t/V) and intercept/slope ratio $[K_{Iald}(1 + k'_7/k'_5)]$ obtained from a plot of E_t/v_0 versus $[ald_0]$ are analogous to $1/V$ and app K_i determined from a Dixon plot of $1/v_i$ versus I (Dixon, 1953). Note that the apparent K_i for v_0 is equal to K_{Iald}, the apparent half-saturation constant for the *rate* of E·adduct formation in the absence of glycolaldehyde turnover (Grimshaw et al., 1990), multiplied by the factor $1 + k'_7/k'_5$ to correct for the steady-state level of E·nucl in the presence of glycolaldehyde turnover.

Equation 14 is also valid for v_{lim}, except that $f^{lim}_{E\cdot nucl}$, the enzyme fraction present as E·nucl when E·adduct formation is at equilibrium, now includes a factor for E·adduct:

$$f^{lim}_{E\cdot nucl} = [E\cdot nucl]_{lim}/[E\cdot nucl]_t = 1/\{1 + ([ald_0]/K_{Iald})(1 + K'_{add})\} \quad (18)$$

where $K'_{add} = [E\cdot adduct]/[E\cdot nucl\cdot ald]$ is the apparent equilibrium constant for adduct formation at the ALR2 active site, as defined in the preceding paper (Grimshaw et al., 1990). Substituting into eq 14, the expression for the *limiting* steady-state rate becomes

$$v_{lim}/E_t = (V/E_t)/\{1 + [ald_0](1 + K'_{add})/K_{Iald}(1 + k'_7/k'_5)\} \quad (19)$$

Equation 19 again has the form of eq 9 with $I = [ald_0]$ and $K_i = K_{Iald}(1 + k'_7/k'_5)/(1 + K'_{add})$. Conversion of eq 19 into the Dixon plot format gives

$$E_t/v_{lim} = E_t/V + [ald_0]E_t/\{V\cdot K_{Iald}(1 + k'_7/k'_5)/(1 + K'_{add})\} \quad (20)$$

The apparent K_i determined from a plot of E_t/v_{lim} versus $[ald_0]$ is thus equal to $K_{Iald}/(1 + K'_{add})$, the apparent half-saturation constant for the equilibrium *amount* of E·adduct formation (i.e., $f_{E\cdot adduct}$) in the absence of glycolaldehyde turnover (Grimshaw et al., 1990), multiplied by the same partition factor $(1 + k'_7/k'_5)$. By taking the ratio of these two apparent K_i values, we eliminate this factor and obtain an expression for K'_{add}:

$$(\text{app } K_i \text{ for } v_0)/(\text{app } K_i \text{ for } v_{lim}) = 1 + K'_{add} \quad (21)$$

According to Scheme I, the steady-state reaction velocity will display an exponential decay from v_0 to v_{lim}. The apparent first-order rate constant for this process

$$k'_{app} = k'_f K_{enol}[ald_0] f'_{E\cdot nucl} + k'_r \quad (22)$$

is analogous to k_{app} determined from the rate of approach to equilibrium for E·adduct formation in the absence of turnover (Grimshaw et al., 1990), with the inclusion of the steady-state partition factor k'_7/k'_5 in the expression for $f'_{E\cdot nucl}$:

$$f'_{E\cdot nucl} = [E\cdot nucl]_{ss}/[E]_t = 1/\{[ald_0]/K_{Iald} + (1 + k'_7/k'_5)\} \quad (23)$$

Substituting for $f'_{E\cdot nucl}$ and rearranging, we obtain

$$k'_{app} - k'_r = k'_f K_{enol} K_{Iald}[ald_0]/\{[ald_0] + K_{Iald}(1 + k'_7/k'_5)\} \quad (24)$$

which has the same form as the Michaelis-Menten equation:

$$v_i = VA/(K_a + A) \quad (3)$$

with $v_i = k'_{app} - k'_r$, $A = [ald_0]$, $V = k'_f K_{enol} K_{Iald}$, and $K_a = K_{Iald}(1 + k'_7/k'_5)$. Thus, $k'_{app} - k'_r$ (i.e., the net contribution of adduct *formation* to k'_{app}) will display saturation by $[ald_0]$ with an apparent half-saturation constant equal to $K_{Iald}(1 + k'_7/k'_5)$ and a maximum value of $k'_f K_{enol} K_{Iald}$, or in double-reciprocal form

$$1/(k'_{app} - k'_r) = (1/k'_f K_{enol} K_{Iald}) + (1/[ald_0])\{(1 + k'_7/k'_5)/k'_f K_{enol}\} \quad (25)$$

Provided k'_r can be measured independently, analysis of the k'_{app} value as a function of $[ald_0]$ allows determination of $K_{Iald}(1 + k'_7/k'_5)$ and k'_f [calculated as (app V)$/K_{Iald}K_{enol}$]. Just as in the absence of glycolaldehyde turnover, K'_{add} can be estimated as (app V)$/k'_r = k'_f K_{enol} K_{Iald}/k'_r = K_{enol} K_{Iald} K'_{eq} = K'_{add}$. In addition to direct measurement of k'_r, the following expression can be derived from eqs 16, 19, and 24

$$k'_r = (k'_{app} v_{lim}/v_0) \quad (26)$$

which relates k'_r to the three experimental parameters k'_{app}, v_{lim}, and v_0.

REFERENCES

Alberty, R. A., & Koerber, B. M. (1957) *J. Am. Chem. Soc. 79*, 6379.

Bohren, K. M., Bullock, B., Wermuth, B., & Gabbay, K. H. (1989) *J. Biol. Chem. 264*, 9547–9551.

Burgner, J. W., II, & Ray, W. J., Jr. (1974) *Biochemistry 13*, 4229–4237.
Burgner, J. W., II, & Ray, W. J., Jr. (1978) *Biochemistry 17*, 1654–1661.
Burgner, J. W., II, Ainslie, G. R., Jr., Cleland, W. W., & Ray, W. J., Jr. (1978) *Biochemistry 17*, 1646–1653.
Cleland, W. W. (1963a) *Arch. Biochem. Biophys. 67*, 104–137.
Cleland, W. W. (1963b) *Arch. Biochem. Biophys. 67*, 173–187.
Cleland, W. W. (1975) *Biochemistry 14*, 3220–3224.
Cleland, W. W. (1979) *Methods Enzymol. 63*, 103–138.
Conrad, S. M., & Doughty, C. C. (1982) *Biochim. Biophys. Acta 708*, 348–357.
Del Corso, A., Barsacchi, D., Giannessi, M., Tozzi, M. G., Camici, M., & Mura, U. (1989) *J. Biol. Chem. 264*, 17653–17655.
Dixon, M. (1953) *Biochem. J. 55*, 107–171.
Dixon, W. J., Ed. (1988) in *BMDP Statistical Software Manual, Vol. 1*, pp 389–416, University of California Press, Berkeley, CA.
Fraenkel-Conrat, H., & Singer, B. (1988) *Proc. Natl. Acad. Sci. U.S.A. 85*, 3758–3761.
Grimshaw, C. E. (1986) *Fed. Proc. 45*, A1500.
Grimshaw, C. E. (1987) *Fed. Proc. 46*, A1756.
Grimshaw, C. E. (1989) *J. Cell Biol. 104*, 401a.
Grimshaw, C. E., Shahbaz, M., Jahangiri, G., Putney, C. G., McKercher, S. R., & Mathur, E. J. (1989) *Biochemistry 28*, 5343–5353.
Grimshaw, C. E., Shahbaz, M., & Putney, C. G. (1990) *Biochemistry* (preceding paper in this issue).
Gutfreund, H., Cantwell, R., McMurray, C. H., Criddle, R. S., & Hathaway, G. (1968) *Biochem. J. 106*, 683–687.
Hermes, J. D., Morrical, S. W., O'Leary, M. H., & Cleland, W. W. (1984) *Biochemistry 23*, 5479–5488.
Mathur, E. J., & Grimshaw, C. E. (1986) *Arch. Biochem. Biophys. 247*, 321–327.
McGhee, J. D., & von Hippel, P. H. (1975) *Biochemistry 14*, 1281–1296.
McKercher, S. R., Mathur, E. J., & Grimshaw, C. E. (1985) *Fed. Proc. 44*, 427.
Morjana, N. A., & Flynn, T. G. (1989) *J. Biol. Chem. 264*, 2906–2911.
Morjana, N. A., Lyons, C., & Flynn, T. G. (1989) *J. Biol. Chem. 264*, 2912–2919.
Neet, K. E., & Ainslie, G. R., Jr. (1980) *Methods Enzymol. 64*, 192–226.
Nishimura, C., Wistow, G., & Carper, D. (1989) *Prog. Clin. Biol. Res. 290*, 211–220.
P-L Biochemicals (1961) Circular OR-18, P-L Biochemicals, Milwaukee, WI.
Schade, S. Z., Lee, S.-M., Williams, T. R., & Doughty, C. C. (1987) *International Workshop on Aldose Reductase Inhibitors*, Dec. 7–10, Honolulu, HI, Abstract C1.2, ICI Pharmaceuticals Group, Cheshire, U.K.
Schade, S. Z., Early, S. L., Williams, T. R., Kézdy, F. J., Heinrikson, R. L., Grimshaw, C. E., & Doughty, C. C. (1990) *J. Biol. Chem. 265*, 3628–3635.
Sogin, D. C., & Plapp, B. V. (1975) *J. Biol. Chem. 250*, 205–210.
Suhadolnik, R. J., Lennon, M. B., Uematsu, T., Monahan, J. E., & Baur, R. (1977) *J. Biol. Chem. 252*, 4125–4133.
Turner, A. J., & Flynn, T. G. (1982) *Prog. Clin. Biol. Res. 114*, 401–402.
Williams, J. W., & Morrison, J. F. (1979) *Methods Enzymol. 63*, 437–467.
Windmuller, H. G., & Kaplan, N. O. (1961) *J. Biol. Chem. 236*, 2716–2726.
Wolff, S. P., & Crabbe, M. J. C. (1985) *Biochem. J. 226*, 625–630.